

Tight Bounds on 3-Neighbor Bootstrap Percolation

by

Abel Emanuel Romer

B.A.Sc., Quest University Canada, 2017

A Thesis Submitted in Partial Fulfillment of the
Requirements for the Degree of

MASTER OF SCIENCE

in the Department of Mathematics and Statistics

© Abel Emanuel Romer, 2022
University of Victoria

All rights reserved. This thesis may not be reproduced in whole or in part, by photocopying or other means, without the permission of the author.

We acknowledge with respect the Lekwungen peoples on whose traditional territory the university stands, and the Songhees, Esquimalt, and WSÁNEĆ peoples whose historical relationships with the land continue to this day.

Tight Bounds on 3-Neighbor Bootstrap Percolation

by

Abel Emanuel Romer

B.A.Sc., Quest University Canada, 2017

Supervisory Committee

Dr. Peter Dukes, Co-Supervisor
(Department of Mathematics and Statistics)

Dr. Jonathan Noel, Co-Supervisor
(Department of Mathematics and Statistics)

ABSTRACT

Table of Contents

Supervisory Committee	ii
Abstract	iii
Table of Contents	iv
List of Tables	v
List of Figures	vi
Acknowledgements	vii
Dedication	viii
Chapter 1 Introduction	1
1.1 Formalizing these observations	2
1.2 Minimum percolating sets and bounds	5
1.2.1 Foundations	5
1.2.2 Additional results	8
Chapter 2 A Recursive Technique	9
2.1 A Helpful Lemma	9
2.2 Examples and Notation	9
2.3 Regional vs. Temporal Infections	9
Chapter 3 A Tight Bound on Grids of Size ≥ 5	10
3.1 Introduction and Definitions	10
3.2 Completeness of Thickness 5	10
3.3 Completeness of Thickness 6	12
3.4 Completeness of Thickness 7	13
3.5 Completeness of Grids of Size ≥ 5	15

Chapter 4	Constructions	16
4.1	Introduction	16
4.2	Useful lemmas and observations	16
4.3	Thickness 1	17
4.3.1	Purina	17
4.3.2	Snakes	18
4.4	Thickness 2	19
4.5	Thickness 3	20
Bibliography		27

List of Tables

Table 1.1 A summary of known bootstrap percolation results for grids and the torus, $r \in \{0, 1, 2, 3, d\}$	5
--	---

List of Figures

Figure 1.1	An arbitrary set of initially infected cells in the 10×10 lattice, and the stages of infection.	1
Figure 1.2	Two lethal sets and their resulting infections after one time-step.	2
Figure 1.3	Percolation time-steps for an arbitrary initial infection on the 5×5 lattice, $r = 2$	6
Figure 1.4	Percolation time-steps for a “spanning” initial infection on the 5×5 lattice, $r = 2$	6
Figure 1.5	A lethal infection on the 8×4 lattice, $r = 2$	6
Figure 3.1	Thickness 6 grids with perfect percolating sets as obtained in lemma 3.5 (left), and divisibility cases of thickness 6 (right). . .	12
Figure 4.1	A perfect percolating set for $(3, 3, 1)$	17
Figure 4.2	A perfect percolating set for $(15, 15, 1)$	18
Figure 4.3	An optimal percolating set for $(5, 5, 1)$	18
Figure 4.4	An optimal percolating set for $(5, 13, 1)$	19
Figure 4.5	An optimal percolating set for $(11, 13, 1)$	19
Figure 4.6	A perfect percolating set for $(3, 12, 2)$	19
Figure 4.7	A proper unfolding of $G = (3, 12, 2)$. Colored rectangles indicate faces of G . Dashed lines indicate that cells appear on different layers.	20
Figure 4.8	A percolating set on the proper unfolding of $G = (3, 12, 2)$	20
Figure 4.9	A perfect percolating set for $(11, 20, 2)$	21
Figure 4.10	A proper unfolding of $G = (11, 20, 2)$. Colored rectangles indicate faces of G . Dashed lines indicate that cells appear on different layers.	21
Figure 4.11	A percolating set on the proper unfolding of $G = (11, 20, 2)$. . .	21
Figure 4.12	A perfect percolating set for $(12, 21, 2)$	22

Figure 4.13	A proper unfolding of $G = (12, 21, 2)$. Colored rectangles indicate faces of G . Dashed lines indicate that cells appear on different layers.	22
Figure 4.14	A percolating set on the proper unfolding of $G = (12, 21, 2)$. . .	22
Figure 4.15	A percolating set on the proper unfolding H' of $G = (15, 23, 3)$.	23
Figure 4.16	A proper unfolding of $G = (15, 23, 3)$. Colored rectangles indicate faces of G	24
Figure 4.17	25
Figure 4.18	26

ACKNOWLEDGEMENTS

DEDICATION

Chapter 1

Introduction

We shall begin this thesis with a puzzle. Consider the lattice depicted in the leftmost diagram of figure 1.1. We refer to the elements of this lattice as *cells*. Suppose we have the capacity to infect some cells (colored red) with a disease, and that this disease will, over a period of time, propagate through uninfected cells of the lattice. Let uninfected cells become infected if they are exposed to at least two infected neighboring cells in the vertical and/or horizontal directions. We say that the initial infection is *lethal* if the entire lattice ultimately becomes infected. Here is the puzzle:

Question. *What is the fewest number of infected cells necessary to spawn a lethal infection?*

Before we present the solution (which is particularly elegant and satisfying, and the reader is encouraged to play around with this problem on their own and get a feel for the behavior), let us take a moment to examine some properties of infectious sets and attempt to characterize what attributes might correspond to lethality. It should not take too long to observe that if an initial infection is in some way “spread too thin,” it will be unable to jump between infected areas, leading to gaps in infection, which we refer to as *immune regions*. The perimeter of the lattice is particularly susceptible to this, as vertices there have fewer neighbors from whom they might be exposed. Heuristically, then, a lethal set must have the ability to effectively span the entire lattice, and must be particularly virulent along the perimeter.

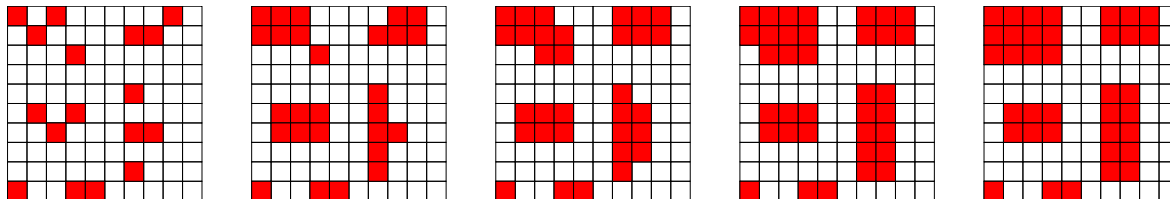


Figure 1.1: An arbitrary set of initially infected cells in the 10×10 lattice, and the stages of infection.



Figure 1.2: Two lethal sets and their resulting infections after one time-step.

At this point, we are able to make some educated guesses regarding the specific structure of sets that are likely to be lethal. In particular, we would like to consider the two starting infections illustrated in figure 1.2. Notice that while figure 1.2 (b) has far fewer perimeter infections, both (a) and (b) manage to form continuous bands of infected cells that appear to span the entire lattice after one step. Indeed, this holds with our notion of immune regions (or lack thereof), and we see that both infections will continue to propagate outwards from these bands until all cells become infected.

It is clear from figure 1.2 that we may obtain lethal sets on the $n \times n$ lattice of size n by simply infecting the diagonal. What is less obvious is whether it is possible to improve upon this result. Perhaps the most natural first attempt at this is to remove an infection from one of the cells along the diagonal. However, this seems to form an immune region around the removed cell. After some experimentation, one begins to believe it impossible to simultaneously satisfy the heuristic that a starting infection must span the lattice, while also using fewer than n initial infections. The question therefore becomes: how do we prove it?

1.1 Formalizing these observations

Before presenting a proof, let us take a moment to formally define the process described above and develop some useful notation. The study of such cellular infection spread in grids (and more generally in graphs) is known in the literature as *bootstrap percolation*, and was introduced in the 1970s by Chalupa et al. [?] as a simplified model for the behavior of ferromagnetic fields. In their original 1979 paper, the authors research the stable structure of probabilistically selected initial infections. While this differs from the problem posed in question 1, the rules for the spread of infection and its broad behavior remain the same. It is worth noting that a large portion of contemporary research on bootstrap problems is focused on questions of probabilistic nature; while these problems are certainly of merit and quite interesting, they do not fall within the scope of this thesis. Rather, we shall focus on those problems where we have specific control over the structure of the initial infections; in particular, we aim to determine

the smallest lethal set on a variety of graph classes.

Let us define our problem in concrete terms. Let G be a graph and $A_0 \subseteq V(G)$ be a set of initially infected vertices. Iteratively, we infect those vertices of G with at least r infected neighbors. For all $t > 0$, let A_t be the set of infected vertices at time step t . We then have

$$A_t = A_{t-1} \cup \{v \in V(G) : |N_G(v) \cap A_{t-1}| \geq r\},$$

where $N_G(v)$ is the set of vertices adjacent to v in G . We define the *closure* of A_0 under r -neighbor bootstrap percolation to be $[A_0] = \bigcup_{t=0}^{\infty} A_t$. We say that A_0 *percolates* or is *lethal* if $[A_0] = V(G)$. We define the smallest percolating set on a graph G under r -neighbor bootstrap percolation by the quantity $m(r, G)$. We note that under these rules, it is not possible for vertices to become uninfected.

In the context of question 1, $G = P_{10} \square P_{10}$, and our diagonal construction shows us that $m(2, G) \leq 10$. In general, we have observed that for $G = P_n \square P_n$, $m(2, G) \leq n$. Now, let us prove that the bound is, in fact, tight.

Proposition 1.1. *For all $n \geq 1$,*

$$m([n]^2, 2) = n.$$

Proof. The upper bound follows from our diagonal construction in figure 1.2 (b). The lower bound is given by the famous “perimeter argument”. Consider the $n \times n$ grid G , given by $G = P_n \square P_n$. Let $A_0 \subseteq V(G)$ be a set of initially infected cells. We claim that the total perimeter of all infected regions in G is monotonically decreasing as a function of the time-step t . Consider an arbitrary healthy cell c . In order for c to become infected, at least two of its edges must abut infected cells. However, this implies that (upon infection of c) these edges are absorbed within the newly expanded infected region, thereby reducing the perimeter of infection by two. As c contains at most two un-absorbed edges, the perimeter of infection cannot increase.

Since a lethal set will infect the entire grid, and therefore have a final perimeter of infection of $4n$, it follows that the perimeter of infection of A_0 must be at least $4n$, and so $m([n]^2, 2) \geq n$. \square

This proof appears in [?], although it has been an established result in bootstrap percolation “folklore” for considerably longer. We should like to make a few additional observations.

First, note that we have used the following three expressions to describe the same graph G :

$$\text{i) } n \times n \quad \text{ii) } P_n \square P_n \quad \text{iii) } [n]^2.$$

The notation in (i) is useful when discussing the shape of low dimensional, asymmetric grids. We use the notation in (ii) to remind readers that the fundamental structure in bootstrap percolation problems is a graph, and to suggest possible extensions of the problem discussed in this thesis to other similar objects. The notation in (iii) is the standard way to describe the vertex set of a grid graph, and can readily be generalized to any dimension d by writing $[n]^d$. In a slight abuse of notation, we use $[n]^d$ to represent the entire graph G , and draw edges between vertices that differ by exactly one in exactly one coordinate.

Second, the fact that we have used the notation $[n]^2$ in Proposition 1.1 suggests that we can generalize to higher dimensional grids $[n]^d$. Indeed, simply observe that for a given hypercube cell to become infected, it must donate at least d of its $2d$ hyperplane faces to the infected region, thereby at most maintaining the current $(d-1)$ -perimeter of infection. The following theorem summarizes this result, which we refer to informally as the *surface area bound* or *S.A. bound*.

Theorem 1.2. *For all $n, d \geq 1$,*

$$m([n]^d, d) = n^{d-1}.$$

The problem of bootstrap percolation was first introduced in the 1970s by Chalupa et al. [?] as a simplified model for the behavior of ferromagnetic fields. In their original paper, the authors describe bootstrap percolation as the stabilization of a probabilistically occupied lattice, where each occupied site must be adjacent to at least m occupied neighbors. A re-rendering of the examples given in the original 1979 paper is presented in figures 1 and 2.

In this original problem, the authors are interested in the structural patterns of these stable arrangements. Put differently, given a set of randomly distributed occupants on a d -dimensional lattice, what configuration can we expect these occupied sites to fall into, subject to the constraint that each occupied site is adjacent to at least m other occupants? In this construction, a probabilistically populated lattice is iteratively depopulated until it reaches a stable state.

Alternatively, we might consider the behavior of a population as it grows, instead of shrinks. In this model, it is useful to consider the population as harboring an infection that steadily spreads from site to site, subject to population density. We shall consider these infections to take place on a graph, with vertices representing members of our population (sites), and edges indicating adjacency. In formal terms: let G be a graph and $A_0 \subseteq V(G)$ be a set of initially infected vertices. Iteratively, at every time step, infect those vertices of G with at least r infected neighbors. For all $t > 0$, let A_t be the set of infected vertices at time step t . We then have

$$A_t = A_{t-1} \cup \{v \in V(G) : |N_G(v) \cap A_{t-1}| \geq r\},$$

	Grids								
r	$[a_1]$	$[a_1] \times [a_2]$	$[n]^2$	$[a_1] \times [a_2] \times [a_3]$	$[n]^3$	\cdots	$\prod_{i=1}^d [a_i]$	$[n]^d$	$[2]^d$
$r = 0$	0	0	0	0	0		0	0	0
$r = 1$	1	1	1	1	1		1	1	1
$r = 2$	$\lceil \frac{a_1-1}{2} \rceil + 1$	$\lceil \frac{a_1+a_2-2}{2} \rceil + 1$	n	$\lceil \frac{a_1+a_2+a_3-3}{2} \rceil + 1$	$\lceil \frac{3(n-1)}{2} \rceil + 1$		$\lceil \frac{\sum_{i=1}^d (a_i-1)}{2} \rceil + 1$	$\lceil \frac{d(n-1)}{2} \rceil + 1$	$\lceil \frac{d}{2} \rceil + 1$
$r = 3$???	???	$\lceil \frac{n^2+2n+4}{3} \rceil^*$	S.A. bound	n^2		???	???	$\lceil \frac{d(d+3)}{6} \rceil$
\vdots						\ddots			
$r = d$???	???	???	???	???		S.A. bound	n^{d-1}	???

Table 1.1: A summary of known bootstrap percolation results for grids and the torus, $r \in \{0, 1, 2, 3, d\}$.

where $N_G(v)$ is the set of vertices adjacent to v in G . We define the *closure* of A_0 under r -neighbor bootstrap percolation to be $[A_0] = \bigcup_{t=0}^{\infty} A_t$. This is analogous to the stable states introduced in [?]. We say that A_0 *percolates* or is *lethal* if $[A_0] = V(G)$. We note that under these rules, it is not possible for vertices to become uninfected.

Perhaps the most natural extremal question regarding r -neighbor bootstrap percolation is that of determining the size of the smallest percolating set $A_0 \subseteq V(G)$, for a given graph G . We represent this quantity by $m(G, r)$. There has been a great deal of work done on establishing the value of $m(G, r)$ for various classes of graphs and values of r (see {citations, citations, etc., etc.}). These results are incompletely summarized in table 1.1, and a selection of particularly noteworthy proofs are presented in detail in the following section.

We end this introduction with the presentation of a delightful question about the cardinality of 2-neighbor percolating sets on the two-dimensional lattice. The interested reader is encouraged to find a solution on their own; however, a proof of the result is presented at the beginning of the following section.

Question. Let (n, n) represent the $n \times n$ lattice, given by $G = P_n \times P_n$. What is $m(n, n, 2)$?

1.2 Minimum percolating sets and bounds

1.2.1 Foundations

Let us build some intuition for the behavior of percolating sets on the two-dimensional lattice. Figure 4.3 illustrates the percolation time-steps for an arbitrary initial infection on the graph $G = P_5 \times P_5$, where $r = 2$. (In general, we shall refer to the d -dimensional lattice with sides a_1, \dots, a_d as the d -tuple (a_1, \dots, a_d) . The standard notation is $\prod_{i=1}^d a_i$.)

Note that this configuration fails to infect the entire grid; that is, the initial infection is not lethal. Heuristically, this appears to be a consequence of the fact that

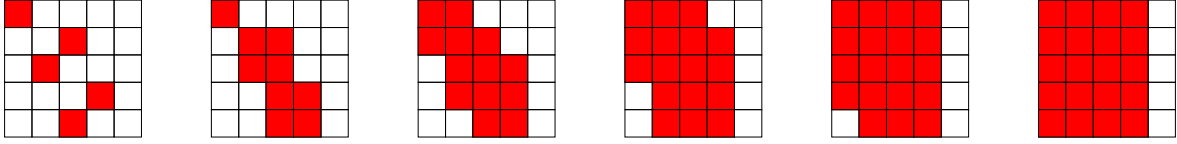


Figure 1.3: Percolation time-steps for an arbitrary initial infection on the 5×5 lattice, $r = 2$.

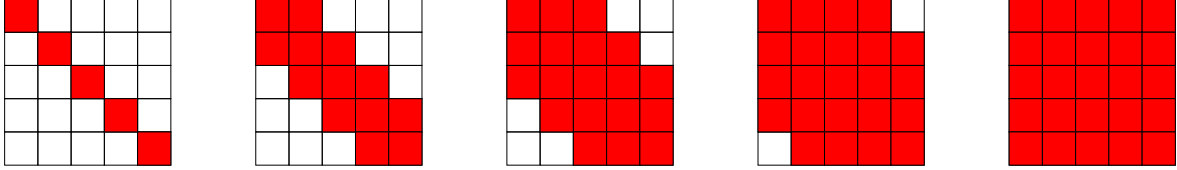


Figure 1.4: Percolation time-steps for a “spanning” initial infection on the 5×5 lattice, $r = 2$.

infected cells are unable to access the healthy cells in the rightmost column. We might, therefore, hypothesize that an initial infection must somehow “span” the entire lattice. A potential “spanning” construction is illustrated in figure 1.4. Observe that at each time-step, the infection spreads out laterally from the initial diagonal. It is a simple exercise to verify that this construction is lethal on all (n, n) grids for $r = 2$. We also note that a similar construction is lethal on all (n, m) grids for $r = 2$ (figure 1.5).

The (n, n) construction can be generalized to any dimension. Specifically, we have:

Proposition 1.3. *For all $n, d \geq 1$,*

$$m([n]^d, d) \leq n^{d-1}.$$

This result has been known since at least Pete [?], although the particular constructions are difficult to render in general. The following proof (appearing in [?], but known in bootstrap percolation “folklore” for much longer) elegantly shows that this bound is tight.

Theorem 1.4. *For all $n, d \geq 1$,*

$$m([n]^d, d) = n^{d-1}.$$

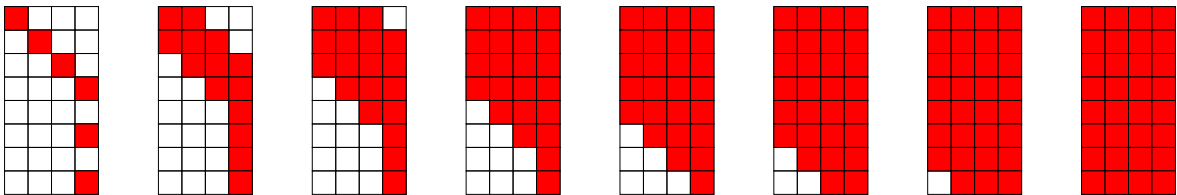


Figure 1.5: A lethal infection on the 8×4 lattice, $r = 2$.

Proof. The upper bound follows from proposition 1.3. The lower bound is given by a generalization of the famous “perimeter argument”. Suppose $d = 2$ and consider an embedding of $G = [n]^d$ in the $n \times n$ grid. Let $A_0 \subseteq V(G)$ be a set of initially infected cells. We claim that the total perimeter of all infected regions in G is monotonically decreasing as a function of the time-step t . Consider an arbitrary healthy cell c . In order for c to become infected, at least two of its edges must abut infected cells. However, this implies that (upon infection of c) these edges are absorbed within the newly expanded infected region, thereby reducing the perimeter of infection by two. As c contains at most two un-absorbed edges, the perimeter of infection cannot increase.

Since a lethal set will infect the entire grid, and therefore have a final perimeter of infection of $4n$, it follows that the perimeter of infection of A_0 must be at least $4n$, and so $m([n]^2, 2) \geq n$.

The same argument generalizes nicely to higher dimensions. Simply observe that for a given hypercube cell to become infected, it must donate at least d of its $2d$ hyperplane faces to the infected region, thereby at most maintaining the current $(d - 1)$ -perimeter of infection. \square

We note that the perimeter argument extends directly to rectangular grids; however, the problem of obtaining tight constructions, should they exist, is largely unsolved and will be the main focus of this thesis. The following proposition, which we refer to informally as the *surface area bound* or *S.A. bound*, provides a lower bound on the size of lethal sets for d -dimensional rectangular grids where $r = d$.

Proposition 1.5. *For $d \geq 1$ and $a_1, \dots, a_d \geq 1$,*

$$m(a_1, \dots, a_d, d) \leq \frac{\sum_{i=1}^d \prod_{j \neq i} a_j}{d}.$$

Proof. Observe that the expression

$$\frac{\sum_{i=1}^d \prod_{j \neq i} a_j}{d}$$

is precisely the high-dimensional perimeter of the grid graph (a_1, \dots, a_d) . The bound follows from the perimeter argument in theorem 1.4. \square

In {some chapter of this thesis}, we will prove that this bound is tight in the case where $d = 3$ and $d_1, d_2, d_3 \geq 8$. We fully expect that this bound can be incrementally diminished; however, we feel that such small improvements do not at this time justify the effort required to obtain additional constructions.

In the remainder of this section, we shall present a number of additional bootstrap percolation results for different classes of grid graphs.

1.2.2 Additional results

Recall from the previous section that $m(n, n, 2) = n$, where the tight construction for the lower bound is given by a diagonal infection expanding laterally outwards. In a paper by Balogh and Bollobas [?], this result is generalized to all d -dimensional hypercubes (a_1, \dots, a_d) , $a_i \geq 1$.

Theorem 1.6. *For $d \geq 1$ and $a_1, \dots, a_d \geq 1$,*

$$m(a_1, \dots, a_d, 2) = \left\lceil \frac{\sum_{i=1}^d (a_i - 1)}{2} \right\rceil + 1.$$

Proof. □

As suggested by table 1.1, general results become quite sparse for $r \notin \{2, d\}$. A nice result from Morrison and Noel resolves the question of $r = 3$ for hypercubes P_2^d of dimension $d \geq 3$.

Theorem 1.7. *For $d \geq 3$ and $a_1 = \dots = a_d = 2$,*

$$m(a_1, \dots, a_d, 3) = \left\lceil \frac{d(d+3)}{6} \right\rceil.$$

Proof. □

However, the issue of determining $m(a_1, \dots, a_d, r)$ is largely unresolved. Furthermore, good lower bounds for $r \neq d$ are conspicuously absent.

Chapter 2

A Recursive Technique

In this chapter, we shall present a technique for constructing large *perfect* grids from smaller perfect grids.

2.1 A Helpful Lemma

Note that there are certain broad structures in a cube that, if present, immediately guarantee it become fully infected. Of greatest importance here is the observation that certain configurations of fully infected sub-cubes (which we shall call blocks) will cause the larger brick to become infected.

Furthermore, note that if each of these smaller blocks is infected with a minimum lethal set, the composite larger brick will also be infected with a minimum lethal set (barring some considerations for divisibility).

2.2 Examples and Notation

2.3 Regional vs. Temporal Infections

Chapter 3

A Tight Bound on Grids of Size ≥ 5

3.1 Introduction and Definitions

Let the ordered tuple (a, b, c) represent the $a \times b \times c$ grid G where $a \geq b \geq c$. We refer to c as the *thickness* of G . For example, the tuple $(5, 3, 3)$ represents a $5 \times 3 \times 3$ grid of thickness 3. We refer to a tuple as *divisible*, or a *divisibility case*, if and only if $ab + bc + ca \equiv 0 \pmod{3}$. If a tuple is divisible and percolates at the lower bound, we refer to it as *perfect*. Observe that the divisibility cases are precisely those grids with integral lower bounds. The divisibility cases of thicknesses belonging to the three residue classes modulo 3 are illustrated in {Figure something}.

In the following lemmas, we use the notation $(a, b, c) + (x, y, z) = (a + x, b + y, c + z)$ to represent respective increases of x , y , and z to the side lengths a , b , and c of G . We note the following:

Remark 3.1. By applying the recursion, $(a, b, c) + (x, y, z)$ percolates at the lower bound when either:

1. $(a, b, c), (a, y, z), (x, b, z), (x, y, c)$ all percolate at the lower bound; or
2. $(x, y, z), (x, b, c), (a, y, c), (a, b, z)$ all percolate at the lower bound.

We shall call a thickness *complete* if it can be shown that all divisibility cases in that thickness are perfect. In this section, we demonstrate that thickness 5, thickness 6 and thickness 7 are all complete. As these belong to the residue classes 2, 0, and 1 modulo 3, respectively, we then use a recursive construction to show that all larger grids are also complete.

3.2 Completeness of Thickness 5

Leveraging {lemmas from earlier chapters yet to be written}, we show that all divisibility cases in thickness 5 percolate at the lower bound.

NOTE: THE FOLLOWING LEMMAS HOLD ASSUMING WE HAVE A GENERAL CONSTRUCTION FOR $(2, 3, 3k)$ FOR ALL k .

Lemma 3.2. *All divisibility cases for grids of the form $(k, 5, 5)$ are perfect.*

Proof. We consider grids obtained from $(5, 2, 2) + (a, 3, 3)$, for $a \equiv 0 \pmod{3}$ and $a > 3$. By remark 3.1, it is sufficient to show that $(5, 2, 2)$, $(5, 3, 3)$, $(a, 2, 3)$, $(a, 3, 2)$ are all perfect. By {a bunch of constructions}, each of these grids percolates at the lower bound for $a > 3$. We therefore obtain all grids of the form $(k, 5, 5)$, for $k > 8$. The only missing grids are $(5, 5, 5)$ and $(8, 5, 5)$, which we have by construction. This completes the proof. \square

Lemma 3.3. *All divisibility cases for grids of the form $(k, 6, 5)$ percolate at the lower bound.*

Proof. We consider grids obtained from $(6, 3, 2) + (a, 3, 3)$, for $a \equiv 0 \pmod{3}$ and $a > 3$. By remark 3.1, it is sufficient to show that $(6, 3, 2)$, $(6, 3, 3)$, $(a, 3, 3)$, $(a, 3, 2)$ are all perfect. By {a bunch of constructions}, each of these grids percolates at the lower bound for $a > 3$. We therefore obtain all grids of the form $(k, 6, 5)$, for $k > 8$. The only missing grid is $(6, 6, 5)$, which we have by construction. This completes the proof. \square

Lemma 3.4. *Thickness 5 is complete.*

Proof. Let $(a, b, 2)$ represent an arbitrary (divisible) grid of thickness 2, and let $x = a \pmod{6}$ and $y = b \pmod{6}$. By {some as of yet unwritten construction}, we have that $(a, b, 2)$ percolates at the lower bound for all $x, y \in \{0, 2, 3, 5\}$, where $x \neq y$. We consider two constructions: $(a, b, 2) + (6, 3, 3)$ and $(a, b, 2) + (6, 6, 3)$.

By item (1) of the remark, in order to show that $(a, b, 2) + (6, 3, 3)$ percolates at the lower bound, it is sufficient to show that $(a, b, 2)$, $(a, 3, 3)$, $(6, b, 3)$, $(6, 3, 2)$ all percolate at the bound. By {more unwritten constructions}, this is true for all $x, y \in \{0, 2, 3, 5\}$, where $x \neq y$, $a, b > 1$, and at least one of $\{a, b\} > 2$. (Note that if $a = 2$, one of the tuples is $(2, 3, 3)$, which does not percolate at the lower bound; we accommodate for this by re-writing $(a, b, 2) + (6, 3, 3)$ as $(a, b, 2) + (3, 6, 3)$.) The resulting tuple $(a', b', 5)$ is a grid of thickness 5, with a' and b' in the same residue class modulo 6, $x, y \geq 8$, and at least one of $\{a', b'\} \geq 9$. From {some figure representing the divisibility cases of thickness 5}, we see that the lower bound on a' and b' omits all grids of the form $(5, 5, k)$ and $(5, 6, k)$, as well as the singular grid $(8, 8, 5)$.

Applying an analogous argument to $(a, b, 2) + (6, 6, 3)$, we must demonstrate that $(a, b, 2)$, $(a, 6, 3)$, $(6, b, 3)$, $(6, 6, 2)$ all percolate at the lower bound. By {some other constructions}, we again find that this holds for all $x, y \in \{0, 2, 3, 5\}$, where $x \neq y$ and $a, b > 1$. This gives all thickness 5 tuples $(a', b', 5)$ with a' and b' in different residue classes modulo 6, where $a', b' \geq 8$.

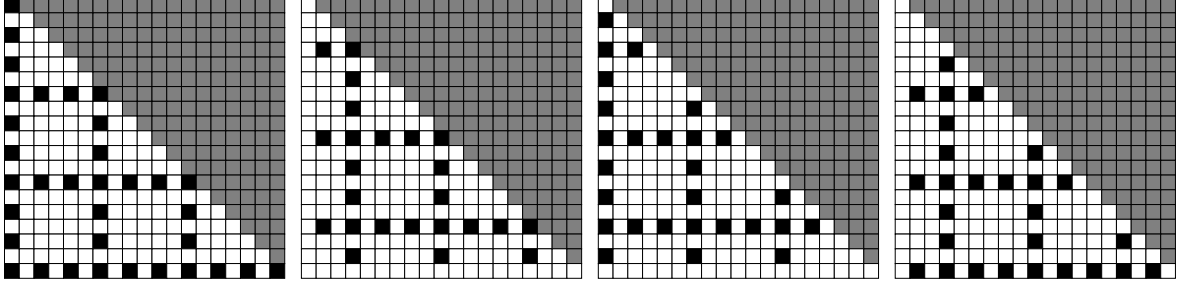


Figure 3.1: Thickness 6 grids with perfect percolating sets as obtained in lemma 3.5 (left), and divisibility cases of thickness 6 (right).

Combining these results, we have completeness for all grids of thickness 5 except those of the form $(5, 5, k)$ and $(5, 6, k)$, and the singular grid $(8, 8, 5)$. By lemmas 3.2 and 3.3, and $\{\text{some construction for } (8, 8, 5)\}$, these cases are also complete, and so thickness 5 is complete. This completes the proof. \square

3.3 Completeness of Thickness 6

We shall show that all grids of thickness 6 can be obtained recursively from $(3n, m, 3)$, where $n, m \equiv 1 \pmod{2}$ (this is that general thickness 3 construction), and one of $\{(3, 3, 3), (6, 6, 3), (6, 3, 3), (3, 6, 3)\}$. We examine each of these cases separately and show that each is complete.

(NOTE (to Peter and Jon): I have struggled a bit with the canonical way to describe grids. I like the tuple representation (a, b, c) where WLOG $a \leq b \leq c$. However, this becomes a bit mucky in the following proofs, because $(3n, m, 3)$ potentially violates this rule if n is large and m is small. To accommodate this, I have written “grids of the form $(a, b, 6)$, where $a \equiv 0 \pmod{6}$ and $b \equiv 0 \pmod{2}$, or $b \equiv 0 \pmod{6}$ and $a \equiv 0 \pmod{2}$,” in an attempt to address the circumstance where the ordering of the tuple is flipped because n is large and m is small. However, I think this may just muddy the waters.)

Lemma 3.5. *All grids of the form $(a, b, 6)$, where $a \equiv 0 \pmod{6}$ and $b \equiv 0 \pmod{2}$, or $b \equiv 0 \pmod{6}$ and $a \equiv 0 \pmod{2}$, percolate at the lower bound.*

Proof. We consider $(3n, m, 3) + (3, 3, 3)$, for $n, m \equiv 1 \pmod{2}$. By remark 3.1, we have that $(3n, m, 3) + (3, 3, 3)$ percolates if $(3n, m, 3), (3n, 3, 3), (3, m, 3), (3, 3, 3)$ all percolate. By construction {yet to be named}, all grids $(a, 3, 3)$ are perfect. Therefore, $(3, 3n, m) + (3, 3, 3)$ is perfect. Note that this grid is of the form $(3k, l, 6)$, where $k, l \equiv 0 \pmod{2}$. This is equivalent to grids of the form $(a, b, 6)$, where $a \equiv 0 \pmod{6}$ and $b \equiv 0 \pmod{2}$, or $b \equiv 0 \pmod{6}$ and $a \equiv 0 \pmod{2}$. This completes the proof. \square

Lemma 3.6. *All grids of the form $(a, b, 6)$, where $a \equiv 3 \pmod{6}$ and $b \equiv 1 \pmod{2}$, or $b \equiv 3 \pmod{6}$ and $a \equiv 1 \pmod{2}$, percolate at the lower bound.*

Proof. We apply the same argument as above, this time considering $(3n, m, 3) + (6, 6, 3)$, for $n, m \equiv 1 \pmod{2}$. Again, by remark 3.1, it is sufficient to show that $(3n, m, 3), (3n, 6, 3), (6, m, 3), (6, 6, 3)$ are all perfect. By {more thickness 3 constructions}, each of these grids percolates at the lower bound. The resulting grid, $(3n, m, 3) + (6, 6, 3)$, for $n, m \equiv 1 \pmod{2}$, is of the form $(a, b, 6)$, for $a \equiv 3 \pmod{6}$ and $b \equiv 1 \pmod{2}$, or $b \equiv 3 \pmod{6}$ and $a \equiv 1 \pmod{2}$. This completes the proof. \square

Lemma 3.7. *All grids of the form $(a, b, 6)$, where $a \equiv 3 \pmod{6}$ and $b \equiv 0 \pmod{2}$, or $b \equiv 3 \pmod{6}$ and $a \equiv 0 \pmod{2}$, percolate at the lower bound.*

Proof. Similarly to the previous proofs, we consider $(3n, m, 3) + (6, 3, 3)$, for $n, m \equiv 1 \pmod{2}$. We show that $(3n, m, 3), (3n, 3, 3), (6, m, 3), (6, 3, 3)$ are all perfect. By the same thickness 3 constructions, each of these grids percolates at the lower bound. Therefore, by remark 3.1, $(3n, m, 3) + (6, 3, 3)$ is perfect. Furthermore, observe that $(3n, m, 3) + (6, 3, 3)$ is of the form $(a, b, 6)$, where $a \equiv 3 \pmod{6}$ and $b \equiv 0 \pmod{2}$. This completes the proof. \square

Lemma 3.8. *All grids of the form $(a, b, 6)$, where $a \equiv 0 \pmod{6}$ and $b \equiv 1 \pmod{2}$, or $b \equiv 0 \pmod{6}$ and $a \equiv 1 \pmod{2}$, percolate at the lower bound.*

Proof. We consider $(3n, m, 3) + (3, 6, 3)$, for $n, m \equiv 1 \pmod{2}$. We show that $(3n, m, 3), (3n, 6, 3), (3, m, 3), (3, 6, 3)$ are all perfect. By {thickness 3 constructions} and remark 3.1, $(3n, m, 3) + (3, 6, 3)$ is perfect. Observe that $(3n, m, 3) + (3, 6, 3)$ is of the form $(a, b, 6)$, where $a \equiv 0 \pmod{6}$ and $b \equiv 1 \pmod{2}$. This completes the proof. \square

Lemma 3.9. *Thickness 6 is complete.*

Proof. All divisibility cases for thickness 6 are grids of the form $(x, y, 6)$ such that at least one of $\{x, y\}$ is congruent to 0 modulo 3. Lemmas 3.5, 3.6, and 3.7 cover all such cases. The result follows. \square

3.4 Completeness of Thickness 7

We show that all divisibility cases for grids of thickness 7 percolate at the lower bound. Observe that divisibility cases for thickness 7 consist of grids of the form $(x, y, 7)$ for x, y in residue classes $\{0, 1, 3, 4\}$ modulo 6. We separate these divisibility cases into the following four categories and show that each category is complete:

1. $(x, y, 7)$ for $x, y \in \{1, 4\}$ and $x \equiv y \pmod{6}$;
2. $(x, y, 7)$ for $x, y \in \{1, 4\}$ and $x \not\equiv y \pmod{6}$;

3. $(x, y, 7)$ for $x, y \in \{0, 3\}$ and $x \equiv y \pmod{6}$;
4. $(x, y, 7)$ for $x, y \in \{0, 3\}$ and $x \not\equiv y \pmod{6}$.

Lemma 3.10. *All grids of the form $(x, y, 7)$ for $x, y \in \{1, 4\}$ and $x \equiv y \pmod{6}$ are complete.*

Proof. Consider the construction $(a, b, 2) + (8, 5, 5)$ for $a, b \in \{2, 5\}$ and $a \not\equiv b \pmod{6}$. Observe that this construction obtains all grids of the form described in (1) above. We show that the grids $(a, b, 2), (a, 5, 5), (8, b, 5), (8, 5, 2)$ are all complete. {The fact that these grids are complete follows from a number of constructions and the observation that thickness 5 is complete.} By remark 3.1, the construction $(a, b, 2) + (8, 5, 5)$ percolates at the lower bound. This completes the proof. \square

Lemma 3.11. *All grids of the form $(x, y, 7)$ for $x, y \in \{1, 4\}$ and $x \not\equiv y \pmod{6}$ are complete.*

Proof. Consider the construction $(a, b, 2) + (5, 5, 5)$ for $a, b \in \{2, 5\}$ and $a \not\equiv b \pmod{6}$. Observe that this construction obtains all grids of the form described in (2) above. We consider the grids $(a, b, 2), (a, 5, 5), (5, b, 5), (5, 5, 2)$. By {known constructions and completeness of thickness 5}, each of these grids is perfect, and so by remark 3.1, $(a, b, 2) + (5, 5, 5)$ percolates at the lower bound. This completes the proof. \square

Lemma 3.12. *All grids of the form $(x, y, 7)$ for $x, y \in \{0, 3\}$ and $x \equiv y \pmod{6}$ are complete.*

Proof. Consider the construction $(a, b, 2) + (6, 9, 5)$ for $a, b \in \{0, 3\}$ and $a \not\equiv b \pmod{6}$. Observe that this construction contains all grids described in (3) above. We consider the grids $(a, b, 2), (a, 9, 5), (6, b, 5), (6, 9, 2)$. Observe that $(3, 9, 5)$ is perfect by construction, and $(a, 9, 5)$ is perfect in general for $a > 3$. Similarly, $(6, 3, 5)$ is perfect by construction, and $(6, b, 5)$ is perfect for all other $b > 3$. Finally, $(a, b, 2)$ and $(6, 9, 2)$ are perfect by construction. Therefore, by remark 3.1, $(a, b, 2) + (6, 9, 5)$ percolates at the lower bound. This completes the proof. \square

Lemma 3.13. *All grids of the form $(x, y, 7)$ for $x, y \in \{0, 3\}$ and $x \not\equiv y \pmod{6}$ are complete.*

Proof. Consider the construction $(a, b, 2) + (6, 6, 5)$ for $a, b \in \{0, 3\}$ and $a \not\equiv b \pmod{6}$. Observe that this construction contains all grids described in (4) above. We consider the grids $(a, b, 2), (a, 6, 5), (6, b, 5), (6, 6, 2)$. Observe that $(3, 6, 5)$ is perfect by construction, and $(a, 6, 5)$ is perfect in general for $a > 3$. Similarly, $(6, 3, 5)$ is perfect by construction, and $(6, b, 5)$ is perfect for all other $b > 3$. Finally, $(a, b, 2)$ and $(6, 6, 2)$ are perfect by construction. Therefore, by remark 3.1, $(a, b, 2) + (6, 6, 5)$ percolates at the lower bound. This completes the proof. \square

Lemma 3.14. *Thickness 7 is complete.*

Proof. By lemmas 3.10, 3.11, 3.12, and 3.13, all divisibility cases for thickness 7 percolate at the lower bound. \square

3.5 Completeness of Grids of Size ≥ 5

We can get completeness in every residue class modulo 3 by simply considering the grids obtained from $(x, y, z) + (3, 3, 3)$.

Chapter 4

Constructions

4.1 Introduction

In this chapter, we present diagrammed proofs of lethal sets that percolate at the lower bound. The proofs are organized by the thickness of the grid. Many of the constructions in the following sections belong to infinite families of either optimal or perfect sets. In this case, we shall examine the grids by region, and observe that certain regions can be expanded to arbitrarily large sizes using mathematical induction.

We shall call a thickness *semi-complete* if all divisibility cases are optimal.

4.2 Useful lemmas and observations

We shall see that similar patterns and structures appear with some regularity in optimal sets. These structures always infect entire regions, and it will be helpful to recognize them within larger grids when they appear.

Lemma 4.1. *Let $G = P_a \square P_b$ be a graph and $S \subseteq V(G)$ be a subset of the vertices of G . Let $G[\bar{S}]$ be the subgraph of G induced by vertices not in S . Then S is a lethal set if and only if $G[\bar{S}]$ is cycle-free, and has no paths between any two boundary vertices.*

Lemma 4.2. *Let G be a rectangular prism (a, b, c) . If a set S is lethal on three mutually orthogonal faces of G , then S is lethal on G .*

Corollary 4.3. *Let G be a grid assembled from sub-grids G_1, \dots, G_k . Let H_1, \dots, H_k be sets satisfying the conditions of lemma 4.2 for sub-grids G_1, \dots, G_k , respectively. Then $H = H_1 \cup \dots \cup H_k$ is a lethal set in G .*

We refer to the union of mutually orthogonal faces of sub-grids G_1, \dots, G_k as a *manifold* of G . Therefore, corollary 4.3 says that if a set H is lethal on the manifold of G , then H is lethal in G . Furthermore, we define a *proper unfolding* of G as a planar representation of the manifold of G . This can be thought of as a special type of folding

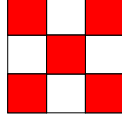


Figure 4.1: A perfect percolating set for $(3, 3, 1)$.

net of G , such that when assembled the resulting structure satisfies the conditions of corollary 4.3.

4.3 Thickness 1

There are two general constructions in thickness 1 that percolate at the surface area bound. The first construction is perfect for all $(2^n - 1, 2^n - 1, 1)$ grids, and originates in a 2021 paper by Benevides et al. [?]. The second construction is optimal for all grids $(a, b, 1)$, where $a \equiv 5 \pmod{6}$, $b \equiv 1 \pmod{2}$, and $a, b \geq 5$. As such grids constitute non-divisibility cases, this construction is not perfect.

4.3.1 Purina

We refer to this construction colloquially as the Purina construction, due to the similarity between its instance on the $(3, 3, 1)$ grid and the logo of the pet food brand. No funding has been offered, but we are open to the possibility. A more extensive discussion on this pattern can be found in [?].

Construction 4.4. *All grids of the form $(2^n - 1, 2^n - 1, 1)$ are perfect.*

Proof. This is a recursive construction built from the base component piece shown in figure 4.1. Note that this $(3, 3, 1)$ construction is lethal under the 3-neighbor bootstrap process, and that it meets the surface area bound:

$$\frac{1}{3} \cdot (ab + bc + ca) = \frac{1}{3} \cdot (9 + 3 + 3) = 5.$$

For larger grids of size $(2^n - 1, 2^n - 1, 1)$, join four copies of $(2^{n-1} - 1, 2^{n-1} - 1, 1)$ about two perpendicular corridors, and infect the vertex at their intersection (figure 4.2). Observe that the resulting set is lethal: each of the four smaller grids is lethal by hypothesis, and the remaining vertices induce a forest with disconnected boundary points, which percolates by lemma 4.1. Furthermore, note that

$$\begin{aligned} \text{S.A.}(2^n - 1, 2^n - 1, 1) &= \frac{1}{3} \cdot (2^{2n} - 1) \\ &= 4 \cdot \frac{1}{3} \cdot (2^{2n-2} - 1) + 1 = 4 \cdot \text{S.A.}(2^{n-1} - 1, 2^{n-1} - 1, 1) + 1, \end{aligned}$$

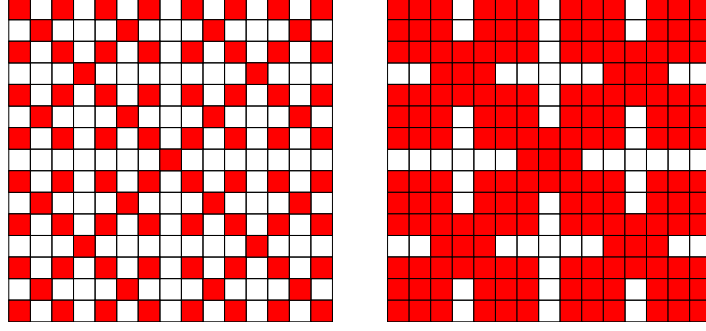


Figure 4.2: A perfect percolating set for $(15, 15, 1)$.

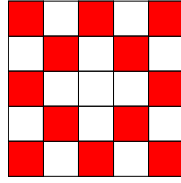


Figure 4.3: An optimal percolating set for $(5, 5, 1)$.

and therefore this construction is perfect. \square

4.3.2 Snakes

As indicated by lemma 4.1, a fundamental characteristic of lethal sets S is the presence of an initially uninfected corridor, bounded by walls of infection. This structure is apparent in the second diagrams of figures 4.2 and 4.5. These corridors correspond to forests in the complement $G[\bar{S}]$ of S . In this subsection, we provide a general method for constructing such corridors in $(a, b, 1)$ grids where $a \equiv 5 \pmod{6}$ and $b \equiv 1 \pmod{2}$.

Construction 4.5. *All grids of the form $(a, b, 1)$, $a \equiv 5 \pmod{6}$, $b \equiv 1 \pmod{2}$, and $a, b \geq 5$ are optimal.*

Proof. For grids of the form $(a, b, 1)$, $a \equiv 5 \pmod{6}$, $b \equiv 1 \pmod{2}$, we construct an optimal infected set and show that it percolates by lemma 4.1. For the base case, consider the $(5, 5, 1)$ grid G illustrated in figure 4.3. Observe that this construction is optimal. Now consider the grid G' resulting from the insertion of a $(5, 2k, 1)$ block, as shown in figure 4.4. Note that the subgraph induced by the uninfected vertices of G' satisfies the conditions of lemma 4.1. Furthermore, note that if any $(5, n, 1)$ grid is optimal, the $(5, n+2, 1)$ grid resulting from such a construction has surface area bound $\text{S.A.}(5, n, 1) + 4$, which agrees with the number of infected vertices.

To extend this construction in the vertical direction, we introduce a kink in the snaking infection. This kink requires six rows to produce a repeating pattern. The structure of this design is shown in figure 4.5. For grids of smaller width, the same

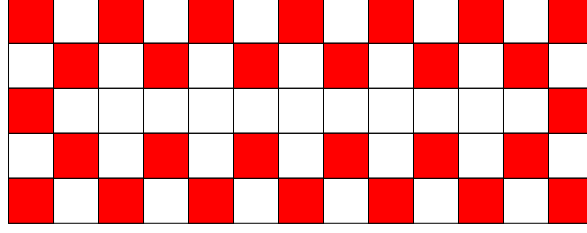


Figure 4.4: An optimal percolating set for $(5, 13, 1)$.

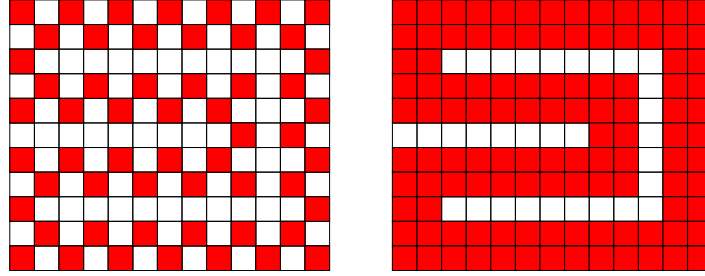


Figure 4.5: An optimal percolating set for $(11, 13, 1)$.

construction gives optimal percolating sets; however, the snaking pattern is increasingly difficult to recognize in thin grids. \square

4.4 Thickness 2

In this section we examine four infinite families of perfect grids. We show that each has a manifold that admits a lethal set of perfect size. We note that such lethal sets are likely to exist for nearly all divisibility cases in thickness two; however, constructions are elusive and those presented here are sufficient to prove the main result of this thesis.

Construction 4.6. *All $(a, 3, 2)$ grids with $a \equiv 0 \pmod{6}$ are perfect.*

Proof. \square

Construction 4.7. *All $(a, 3, 2)$ grids with $a \equiv 0 \pmod{6}$ are perfect.*

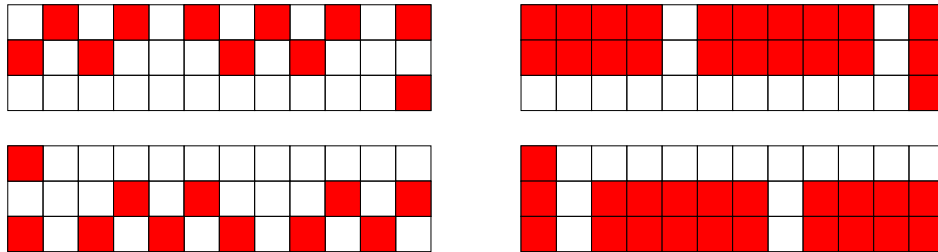


Figure 4.6: A perfect percolating set for $(3, 12, 2)$.

Figure 4.7: A proper unfolding of $G = (3, 12, 2)$. Colored rectangles indicate faces of G . Dashed lines indicate that cells appear on different layers.

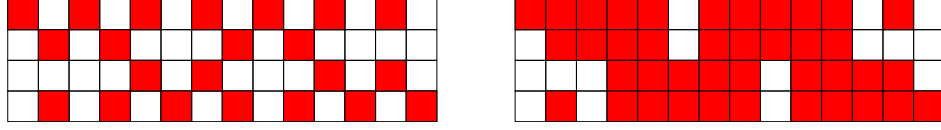


Figure 4.8: A percolating set on the proper unfolding of $G = (3, 12, 2)$.

Proof.

□

Construction 4.8. All $(a, b, 2)$ grids with $a, b \in \{2, 5\} \pmod{6}$ and $a \not\equiv b \pmod{6}$ are perfect.

Proof. Let G be an $(a, b, 2)$ grid with $a, b \in \{2, 5\} \pmod{6}$ and $a \not\equiv b \pmod{6}$, and let H be an unfolding of G (figure 4.10). We show that this unfolding is proper, and that it admits a perfect lethal set.

The above construction holds for $a \geq 11$ and $b \geq 8$. SAY SOMETHING ABOUT THE MISSING CASES.

□

Construction 4.9. All $(a, b, 2)$ grids with $a, b \in \{0, 3\} \pmod{6}$ and $a \not\equiv b \pmod{6}$ are perfect.

Proof. Consider the $(21, 12, 2)$ grid G shown in figure 4.12. Let H be a unfolding of G (figure 4.13). Observe that H is proper: three mutually orthogonal faces of G_1 are shown by blue, green and dashed red regions, and mutually orthogonal faces of G_2 are shown by the red, green and dashed blue regions. We show that H admits a lethal set of size $\text{S.A.}(12, 21, 2) = 106$. Consider such a set, as shown in figure 4.14. (Observe that this is the same set as shown in figure 4.12.) By lemma 4.1, this set percolates with the exception of two C_4 s in the top and bottom of the grid. However, notice that one of these cells is a duplicate of an already infected cell. (This duplication is a consequence of the proper unfolding of G .) Therefore, H admits a lethal set, and by corollary 4.3, G is perfect.

For all larger grids, observe that the snaking corridor in the left side G can be extended by multiples of 6 in both the x and y directions. These resulting grid still percolates under lemma 4.1. A simple calculation verifies that such an alteration produces initial infections at the surface area bound.

□

4.5 Thickness 3

Construction 4.10. All $(a, b, 3)$ grids G with $a \equiv 3 \pmod{6}$ and $b \equiv 1 \pmod{2}$ are perfect.

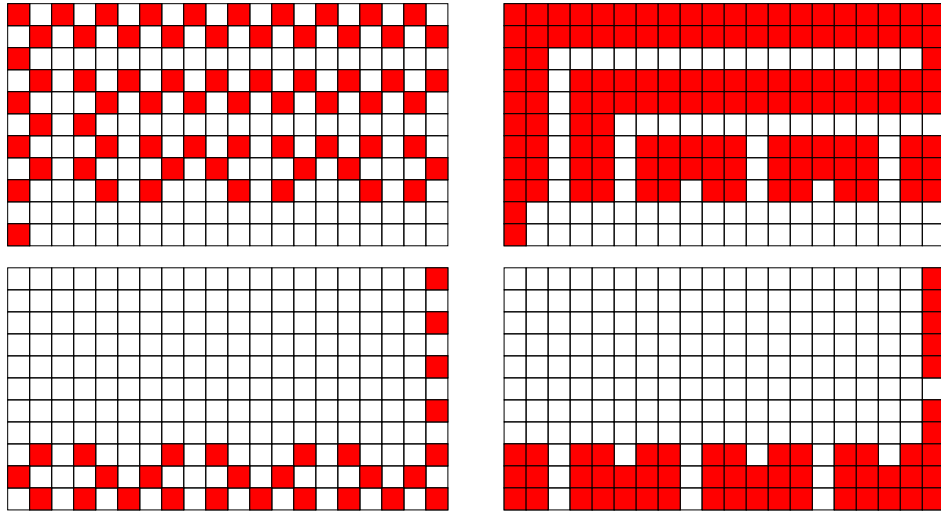


Figure 4.9: A perfect percolating set for $(11, 20, 2)$.

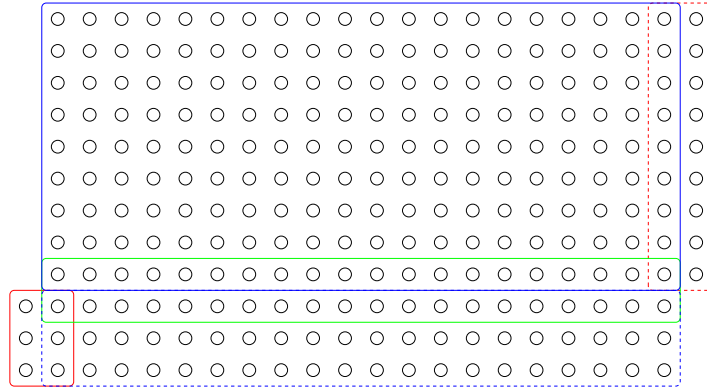


Figure 4.10: A proper unfolding of $G = (11, 20, 2)$. Colored rectangles indicate faces of G . Dashed lines indicate that cells appear on different layers.

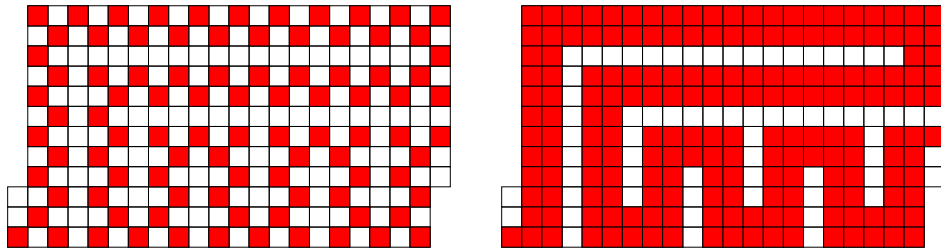


Figure 4.11: A percolating set on the proper unfolding of $G = (11, 20, 2)$.

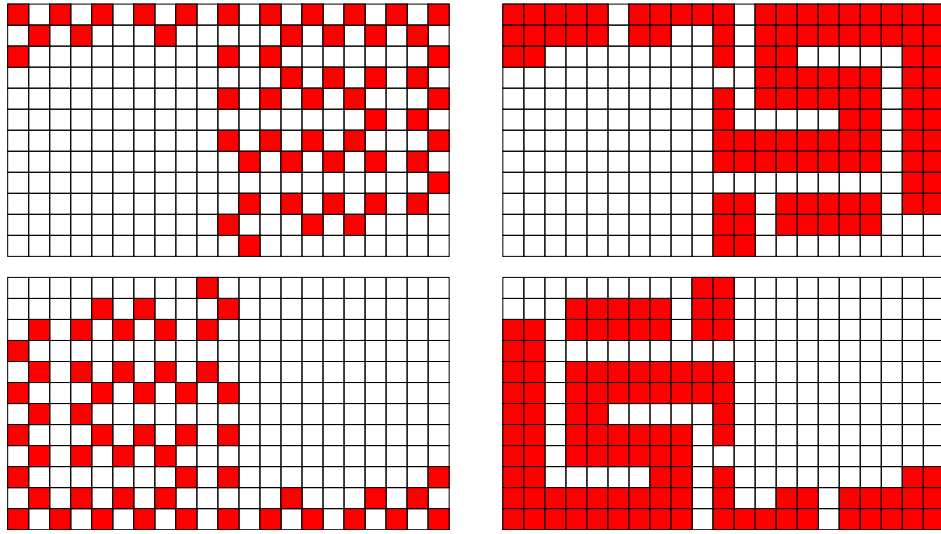


Figure 4.12: A perfect percolating set for $(12, 21, 2)$.

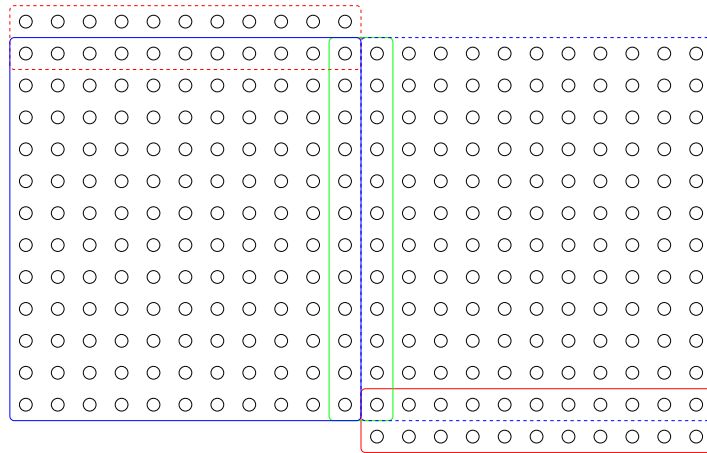


Figure 4.13: A proper unfolding of $G = (12, 21, 2)$. Colored rectangles indicate faces of G . Dashed lines indicate that cells appear on different layers.

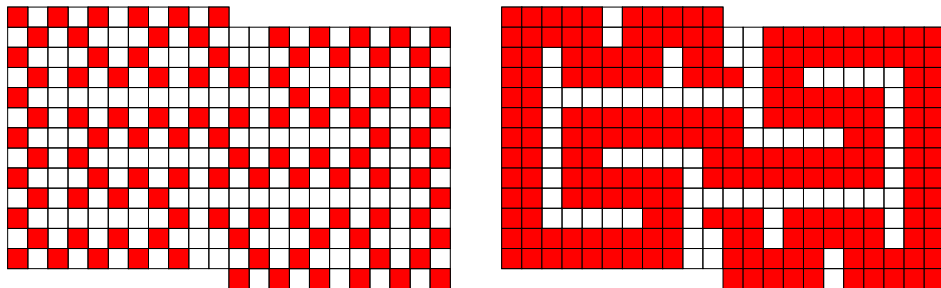


Figure 4.14: A percolating set on the proper unfolding of $G = (12, 21, 2)$.

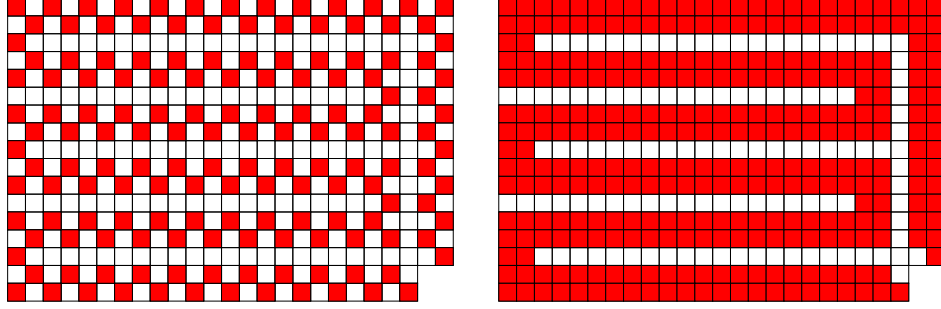
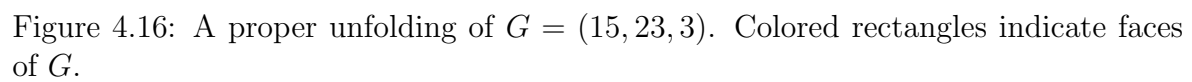


Figure 4.15: A percolating set on the proper unfolding H' of $G = (15, 23, 3)$.

Proof. Consider the grid $H = (a + 2, b + 2, 1)$, and observe that such a grid admits an optimal percolating set by construction 4.5. Note that

$$\text{SA}(a, b, 3) = \lceil \text{SA}(a + 2, b + 2, 1) \rceil - 3.$$

We show that an unfolding of G can be obtained from a simple augmentation of H . Let H' be the grid obtained by deleting the four vertices in the bottom, right-most corner of H (see figure 4.15). Consider the folding pattern illustrated in figure 4.16, and observe that the pairs of vertices adjacent to the deleted region are duplicates of each other. (In other words, consider folding up the red and green regions in figure 4.16, and notice that this operation causes vertices to overlap.) Taking this into account, the unfolding of G percolates by lemma 4.1. Since H admits an optimal percolating set of size $\lceil \text{SA}(a + 2, b + 2, 1) \rceil$, and precisely 3 of the vertices deleted from H to obtain H' were infected, it follows that the unfolding of G percolates at the lower bound. Finally, by lemma 4.2, since the unfolding of G is proper and percolates at the lower bound, G is perfect. \square



	1		1		1		1	
19	18	17		1		1		1
	5	16	15	14	13	12	1	
1	4	5		1		11		1
	1		1		1	12	13	14
1		1	6	7	8	13	14	15

21		21	22	23	24	25	26	27
20	19	20	21	22	23	24	25	26
1		17	18	19	20	21	22	23
	3	6	7	8	9	10	1	
1	2	3	4	1		1		1
	1		5		1		1	

Figure 4.17

[illegible]

81		81	82	83	84	85	86	87	88	89	90	91	92	93	94	95	96	97	98	99	100	101	102	103	104	105	106	107	108	109	110	111
80	3	80	81	82	83	84	85	86	87	88	89	90	91	92	93	94	95	96	97	98	99	100	101	102	103	104	105	106	107	108	109	110
79		79	80	81	82	83	84	85	86	87	88	89	90	91	92	93	94	95	96	97	98	99	100	101	102	103	104	105	106	107	108	109
78	3	78	79	80	81	82	83	84	85	86	87	88	89	90	91	92	93	94	95	96	97	98	99	100	101	102	103	104	105	106	107	108
77		77	78	79	80	81	82	83	84	85	86	87	88	89	90	91	92	93	94	95	96	97	98	99	100	101	102	103	104	105	106	107
76	5	76	77	78	79	80	81	82	83	84	85	86	87	88	89	90	91	92	93	94	95	96	97	98	99	100	101	102	103	104	105	106
75		75	76	77	78	79	80	81	82	83	84	85	86	87	88	89	90	91	92	93	94	95	96	97	98	99	100	101	102	103	104	105
74	3	74	75	76	77	78	79	80	81	82	83	84	85	86	87	88	89	90	91	92	93	94	95	96	97	98	99	100	101	102	103	104
73		73	74	75	76	77	78	79	80	81	82	83	84	85	86	87	88	89	90	91	92	93	94	95	96	97	98	99	100	101	102	103
72	3	72	73	74	75	76	77	78	79	80	81	82	83	84	85	86	87	88	89	90	91	92	93	94	95	96	97	98	99	100	101	102
71		71	72	73	74	75	76	77	78	79	80	81	82	83	84	85	86	87	88	89	90	91	92	93	94	95	96	97	98	99	100	101
70	5	70	71	72	73	74	75	76	77	78	79	80	81	82	83	84	85	86	87	88	89	90	91	92	93	94	95	96	97	98	99	100
69		69	70	71	72	73	74	75	76	77	78	79	80	81	82	83	84	85	86	87	88	89	90	91	92	93	94	95	96	97	98	99
68	67	68	69	70	71	72	73	74	75	76	77	78	79	80	81	82	83	84	85	86	87	88	89	90	91	92	93	94	95	96	97	98
1		65	66	67	68	69	70	71	72	73	74	75	76	77	78	79	80	81	82	83	84	85	86	87	88	89	90	91	92	93	94	95
	3	6	7	8	9	10	11	12	13	14	15	16	17	18	19	20	21	22	23	24	25	26	27	28	29	30	31	32	33	34	1	
1	2	3	4	1		1		1	2	1		1		1	2	1		1		1	2	1		1		1	2	1		1		1
	1		5		1		1		3		1		1		3		1		1		3		1		1		3		1		1	

Figure 4.18

Bibliography

- [1] A. P. Dove, J. R. Griggs, R. J. Kang, and J.-S. Sereni. Supersaturation in the boolean lattice. 2013.